PCCP

Accepted Manuscript

ROYAL SOCIETY OF CHEMISTRY

www.rsc.org/pccp

Physical Chemistry Chemical Physics
CREATED USING THE RSC LaTeX PCCP ARTICLE TEMPLATE – SEE www.rsc.org/electronicfiles FOR DETAILS
ARTICLE TYPE
www. rsc.org/xxxxxx | XXXXXXXX

Growth of Sub-Nanometric Palladium Clusters on Boron Nitride Nanotubes: A DFT Study

Roberto Schimmenti, Remedios Cortese, Francesco Ferrante, Antonio Prestianni, and Dario Duca*

Received Xth XXXXXXXXXX 20XX, Accepted Xth XXXXXXXXX 20XX
First published on the web Xth XXXXXXXXXX 200X
DOI: 10.1039/b000000x

Abstract A QM/MM investigation is reported dealing with the nucleation and growth of small palladium clusters, up to Pd_8, on the outer surface of a suitable model of boron nitride nanotube (BNNT). It is shown that the BNNT could have a template effect on the cluster growth, which is due to the interplay between Pd-N and Pd-Pd interactions as well as to the matching of the B_3N_3 ring and the Pd(111) face arrangement. The values for the clusters adsorption energies reveal a relatively strong physisorption, which suggests that in particular conditions the BNNTs could be used as supports for the preparation of shape-controlled metal clusters.

1 Introduction

Graphene and carbon nanotube (CNT) like systems have gained high interest in a wide range of fields such as electrochemistry,[1] optoelectronics,[2] catalysis[3] and many others.[4] Beside the Group 14 congeners of CNTs and graphene (*i.e.* silicene and germanene) other layered materials have been exploited to reproduce sheet and tubular structures.[5] Among these, boron nitride based nanotube (BNNT) showed really interesting properties such as high chemical and thermal stability as well as great mechanical strength and high thermal conductivity;[6–9] these features make them especially suitable for high temperature technologies and catalysis. Indeed, while it's reported that for common catalyst supports, such as γ-Al_2O_3, a partial sintering of dispersed metals occurs, the BNNT materials should not affect the catalyst dispersion due to their thermal properties and the lack of acidic sites.[10] Moreover, in opposition to the wide majority of catalytic supports, BNNTs are hydrophobic, thus suggesting the possibility to use them in reactions were the presence of water or moisture could influence the catalyst stability and activity.[11]

BNNTs supported metal nanoparticles have been studied as catalysts for the selective oxidation of lactose, showing high activity and selectivity;[12] for this and other related reactions, namely the carbohydrate hydrogenations,[13] it has been showed that the chemical nature of the support could affect the degree of size and dispersion of the nanoparticles, ruling the reaction activity and selectivity. In fact, achieving a well established procedure for the synthesis of shape and size-controlled clusters is a widely discussed topic in literature. The most recent advances in this field claim for a polymer-free synthesis of metal nanoparticles. A well known approach exploits the template action of organic-molecule scaffolds in order to achieve the desired size of the nanoparticles.[14] From this point of view the honeycomb structure of the B_3N_3 rings in the BNNT could generate interesting template effects toward sub-nanometric metal clusters. A computational study could actually elucidate how the metal-BNNT interactions might affect growing and shaping of the nanoparticles. Focusing on this, some studies concerning the adsorption of a single transition metal atom, with particular interest for palladium, have been already carried out.[15] However, to the best of our knowledge, scarce attention has been, up to now, devoted to unravel the growth mechanism of palladium clusters on BNNT. In the present investigation, the interaction and growth of small palladium clusters (from Pd_2 to Pd_8) on a single walled BNNTs have been analyzed by employing computational modeling. Aims were mostly related i) to the understanding of the structural properties characterizing the Pd_n/BNNT systems and ii) to evaluate the potential templating effect of the BNNT support on the cluster shape.

2 Computational Details

The calculations were performed by means of the Gaussian 09 package.[16] Except from few explicited cases, a QM/MM approach exploiting the 2-layer ONIOM method[17] was employed for all the calculations. According to this approach, we chose the Universal Force Field (UFF)[18] as low accuracy method and DFT as the high accuracy one. For the latter, the Coulomb-Attenuated CAM-B3LYP hybrid exchange-correlation functional was used. The Los Alamos LANL2 effective core potential with the corresponding double-ζ basis

[a] *Dipartimento di Fisica e Chimica, Università degli Studi di Palermo, Viale delle Scienze, Parco d'Orleáns II, Palermo, Italy. Fax: +39 091 23860815; Tel: +39 091 23897975; E-mail: dario.duca@unipa.it*

set was employed for the Pd atoms while for the B and N atoms the Dunning D95V basis set was used.

The ONIOM model system is a circumcoronene-like $B_{27}N_{27}$ portion of a (12,12) armchair single walled BNNT, formed on the whole by 12 unit cells. This was chosen on the ground of test calculations involving two different model system sizes — namely, $B_{27}N_{27}$ and $B_{48}N_{48}$ — and the largest cluster used in this investigation, the Pd_8 one, whose properties should be reasonably the most affected by the model system dimension. The Pd_8 adsorption energy was evaluated on both these model systems and the difference between the two results was negligible, being *ca.* 10 kJ mol^{-1}. Therefore, the $B_{27}N_{27}$ model system was used in order to optimize the computational efficiency. Since the calculations are not periodic, the dangling bonds on the terminal sides of the nanotube were saturated with hydrogen atoms.

In order to determine the electronic ground state of the different systems, a full geometry relaxation was carried out on a number of models resulting from the adsorption on the BNNT of one Pd atom (Pd_1) and of all the studied palladium clusters, from Pd_2 to Pd_8, considering the possibility of several configurations and performing all the calculations in the singlet, triplet and quintet spin multiplicities. The nature of minimum on the potential energy surface of an optimized structure was always checked by the calculation and inspection of the harmonic vibrational frequencies. The adsorption energy of a Pd_n cluster on the BNNT was obtained through the general formula

$$\Delta E_n^{Ads} = E_{Pd_n/BNNT} - E_{BNNT} - E_{Pd_n} \quad (1)$$

where $E_{Pd_n/BNNT}$ is the total energy of the supported cluster system, E_{BNNT} the energy of the pristine BNNT and E_{Pd_n} the energy of the isolated Pd_n cluster at the same level of theory in its most stable spin multiplicity, which is the singlet for Pd_1, the triplet for Pd_n ($n = 2-7$) and the quintet for Pd_8. For the Pd_1/BNNT system, the BSSE has been estimated applying the counterpoise method [19] on the solely model system of the ONIOM scheme, saturating with hydrogen atoms the dangling bonds on the edge.

3 Results and Discussion

The analysis of the nucleation and growth mechanisms of metal atoms to form clusters on surfaces could be a really expensive computational task. Indeed, depending on the number of metal atoms considered and on the chemical nature of the support surface, the number of different metal-atoms/surface-sites combination could become prohibitively high.

[Fig. 1 about here.]

Taking into account the boron nitride nanotube, whose optimized structure is depicted in Fig. 1, five possible adsorption sites for one metal atom can be easily recognized, namely the boron and nitrogen atop sites, the axial and zig-zag bridge sites and the center of the B_3N_3 ring. As a consequence, even the introduction of a second metal atom causes a large increase of the number of the different configurations that should be explicitly considered. In the present case, however, the two different bridge sites might be considered as equivalent. This approximation, substantiated by the slight dependence of the adsorption energies from the adsorption surface sites that characterize the transition metals on BNNTs, [15] was useful to capture information in the most complicated cases. In view of this, a peculiar strategy was adopted for modeling the palladium cluster growth. At the n-th step of the growth algorithm employed, a pair of Pd_n/BNNT systems were actually generated by adding a Pd atom in two different ways to the most stable of the available Pd_{n-1}/BNNT structures. In the first case, a site at the center of an exposed Pd_{n-1} cluster face, far from the support, was chosen; in the second, the additional Pd was placed in such a way to assure interactions both with the already adsorbed cluster and the BNNT surface. A representation of this procedure is reported in Scheme 1. By using this protocol, it has been possible to discriminate the contributions given to the system stability by the cooperative or competitive metal-metal and metal-support interactions; the interplay between them indeed should orient toward vertical (metal-driven) or horizontal (support-driven) growth of the cluster.

The single palladium atom adsorbs on the BNNT by a N-atop coordination, showing an adsorption energy of 58.6 kJ mol^{-1} (36.9 kJ mol^{-1} after the BSSE correction) and a Pd–N interaction distance of 2.28 Å. This kind of interaction between palladium and nitrogen has been already described by Koitz et al. [20] in a computational investigation of the BN-sheet growth on the surface of different transition metals.

The optimized structures that we considered relevant for describing the properties of the palladium cluster on the boron nitride nanotube, Pd_n/BNNT (n = 2-4), are displayed in Figure 2. When a second metal atom is added to the monometallic system to form the Pd_2 dimer, the configuration with the singlet spin multiplicity state is characterized by an adsorption energy of 96.5 kJ mol^{-1} while it shows one BN-bridge and one N-atop coordinated palladium atom (see Figure 2a). In the triplet state each palladium atom is instead N-atop coordinated to two different nitrogen atoms (Figure 2b), being however 71.8 kJ mol^{-1} less stable than in the singlet state. The latter thus becomes the most stable multiplicity state after Pd_2 adsorption, in line with an already reported result concerning the interaction of a palladium dimer with the phenyl rings of hypercrosslinked polystyrene. [21] Of course, the geometry and the spin state adopted by the BNNT adsorbed palladium dimer are the result of the balance among the Pd-Pd, the Pd-N and the Pd-B interactions. With respect to the isolated palladium dimer, the Pd-Pd interaction actually seems unchanged in the

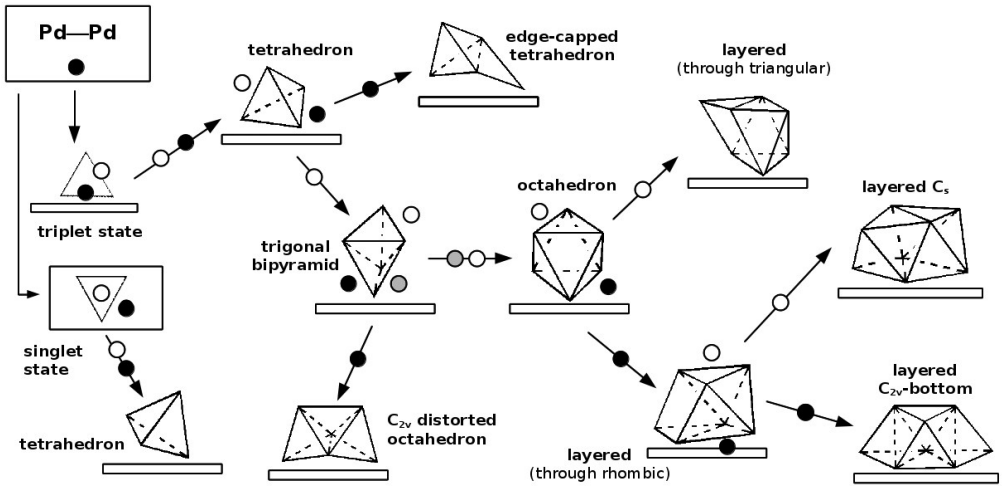

Scheme 1 Algorithm used for the Pd cluster growth on BNNT support: $Pd_{n-1} + Pd \rightarrow Pd_n$; white circles represent new Pd atoms placed on preexisting Pd_{n-1} faces, not in contact with the support surface; the black circles, conversely, represent new Pd atoms placed at the border between the adsorbed Pd_{n-1} cluster and the support. The most stable Pd_n cluster formed, was always chosen. The optimized geometry of the cluster in a given Pd_n/BNNT system is depicted by the representative polyhedron and identified according to the name used throughout the text; BNNT is schematically shown.

triplet spin state as well as the corresponding bond distance (2.53 Å). Clearly, the longer bond in the singlet Pd_2 (2.80 Å) allows a better interaction with the BN rings, as witnessed by the smaller Pd-N bond distances reported in Table 1.

[Fig. 2 about here.]

[Table 1 about here.]

The Pd_3/BNNT system, in the triplet state, shows two Pd atoms interacting atop with two N atoms; the optimized structure of the singlet state cluster, which is less stable by 23.8 kJ mol^{-1} with respect to the triplet, conversely shows, for all the metal atoms, a BN-bridge coordination (Figure 2c). In the triplet state, the cluster retains the isosceles triangular geometry found for the unsupported Pd_3 case, with the same spin multiplicity, but it can be also observed a shortening of the bond between the Pd atoms interacting with the BNNT surface and the concomitant increase of the other two Pd-Pd bonds. On the other hand, the supported Pd_3 in the singlet state shows three different Pd-Pd distances, whereas *in vacuo* the singlet has an equilateral triangular geometry with the Pd-Pd distances equal to 2.55 Å (Table 1) and is 46.4 kJ mol^{-1} less stable than the triplet. So, although its geometry is subjected to distortion, the singlet multiplicity of Pd_3 is slightly stabilized when the cluster is adsorbed on BNNT. The increased stability of the singlet state is imputable to the increased number of interactions occurring with the B_3N_3 ring: in the singlet geometry the Pd_3 cluster indeed lies on the support surface whereas in the triplet only two atoms of the cluster, as it was found for the Pd dimer, interact with it (Figure 2d). Considering the small energy gap between the two multiplicity states, both the adsorption geometries of Pd_3 were included in the following growth scheme.

It is well known that the Pd_4 cluster exhibits two stable *in vacuo* structures: one is square planar with D_{4h} symmetry and one, which is the most stable, a slightly distorted tetrahedron.[22,23] Of course, adsorption processes could affect both the geometry and the intrinsic energy order of these structures. The supported cluster, either in the singlet or in the triplet spin states, shows always a tetrahedral geometry, irrespective of the multiplicity of the starting Pd_3 structure. However, now the triplet multiplicity is by far the preferred one, being 82.1 kJ mol^{-1} more stable than the singlet, which therefore will not be further discussed. The tetrahedral cluster can interact by different binding modes with the BNNT. A single Pd vertex interacts N-atop with the support, or a Pd-Pd edge interacts with two different sites of the BNNT resulting in a coordination that might show an N-atop/BN-bridge or N-atop/N-atop configuration (Figure 2e,f).

As a matter of fact, all these adsorption geometries are approximately isoenergetic, with interaction energies of 147.4 kJ mol^{-1}, 148.5 kJ mol^{-1}, and 152.3 kJ mol^{-1}, respectively. The geometry of the adsorbed Pd_4 clusters is essentially the same,

irrespective of the adsorption mode (see Table 1). When the Pd_4 interacts by only one metallic center a stronger Pd-N interaction can be observed, along with a bond distance of 2.38 Å while, when it interacts by two metallic centers, the double Pd-N interaction is weakened, which results in longer bond distances: 2.58 Å for the N-atop/BN-bridge, 2.46 Å for the N-atop/N-atop. It has to be stressed that the optimization procedure leads to the tetrahedral adsorbed configurations, even considering a planar D_{4h} Pd_4 as starting point. Therefore, it is reasonable to believe that a square planar arrangement of palladium atoms may not occur on the BNNT, a hint that the BNNT surface could control the morphology of the subnanoparticle.

Clearly, the geometry and the interaction energy of the adsorbed cluster should result from the interplay of the Pd-Pd interactions and of the Pd-B and Pd-N ones. Besides, according to Zhang and Alexandrova,[22] which showed that the adsorption of small palladium clusters on TiO_2 is mainly controlled by the matching of the symmetry of the cluster with the local surface morphology, also the BNNT support could be able to rule the final cluster symmetry.

The larger Pd_n (n=5-8) clusters are characterized by several geometries, which were already treated in the literature using different computational methods.[21,24–26] The corresponding energy differences associated to the various geometries of a Pd_n species, when optimized *in vacuo*, can be quite small. As regard the Pd_5 cluster, it was reported that the energy differences of the three most stable configurations – namely, square pyramidal, edge-capped tetrahedral and trigonal bipyramidal – are within a range of 30 kJ mol^{-1}, according to the results obtained by multi-reference *ab initio* methods. The same structures were here obtained by the growth algorithm, both in singlet and triplet spin states on BNNT and, for the sake of comparison, also *in vacuo* at the CAM-B3LYP level. In each case, the triplet state was the most stable (*ca.* 90 kJ mol^{-1} lower in energy than the singlet) while the trigonal bipyramidal geometry was found to be the one energetically preferred both on BNNT (the adsorption geometry is shown in Figure 3a, being its adsorption energy 68.3 kJ mol^{-1}) and *in vacuo*. The supported Pd_5 cluster shows two palladium atoms interacting N-atop/N-atop with the BNNT support: the two Pd-N distances were 2.38 Å, while the Pd(1)-Pd(2) one was 2.58 Å, being Pd(1) and Pd(2) the atoms directly bonded.

[Fig. 3 about here.]

When adsorbed on BNNT, the Pd_5 edge-capped tetrahedral cluster (Figure 3b) resulted 27.7 kJ mol^{-1} less stable than the trigonal bipyramidal reference, characterized by a triplet spin state. Interestingly, while the Pd_5 edge-capped tetrahedral structure was previously reported as a saddle point in the PES of the isolated Pd_5 cluster,[24] it is a local minimum when interacting with BNNT. In fact, according to the CAM-B3LYP results, the edge-capped tetrahedral Pd_5 geometry is not a stationary point in the isolated state, since it invariably converts to the trigonal bipyramidal structure after geometry optimization. On the other hand, although it is described as a minimum in the isolated state, with an energy 29 kJ mol^{-1} higher than that of the trigonal bipyramidal structure, the square pyramidal Pd_5 is a saddle point in the Pd_5/BNNT triplet surface. This evidence also suggests that the support should be able to affect the cluster energetics and growth. Noticeably, in the singlet surface of Pd_5/BNNT, the square pyramidal structure is a minimum, being however its energy 81 kJ mol^{-1} higher than that of the ground state.

Two optimized minima characterize the supported Pd_6 cluster, both showing octahedral geometries: one regular and the other very distorted. The first, which in the triplet state is 89.9 kJ mol^{-1} more stable than the singlet, adsorbs through a triangular face (Figure 3c). The second, characterized by a C_{2v} symmetry, interacts N-atop/N-atop (Figure 3d). Also in the distorted Pd_6 cluster, the triplet is more stable (by 78.8 kJ mol^{-1}) than the singlet. The regular octahedral geometry, which has an adsorption energy of 70.3 kJ mol^{-1}, is 12.0 kJ mol^{-1} more stable than the C_{2v} one. This energy difference is almost the same of that calculated by Ni and Zheng,[27] at the RPBE level, for the isolated Pd_6. However, according to our calculation, the *in vacuo* C_{2v} isolated species does not exist since it spontaneously converts to the octahedral one. It is worth noting (see Figure 3c) the complementarity of one of the octahedral Pd_6 faces with the three nitrogen atoms of the B_3N_3 ring. This, as might be expected, could rule a better interaction of the Pd cluster with the BNNT surface. Then, comparing the Pd-Pd bond distances of this face with those of the opposite one, a small deformation of the octahedron can be noticed: the interacting face experiences in the average a Pd-Pd bond lengthening of 0.1 Å while the opposite face results slightly shrunken. Again, this is determined by efficient Pd_6-BNNT interactions, in details two N-atop interactions (being the Pd-N distances equal to 2.45 and 2.48 Å) and a bridge one (being the Pd-N and Pd-B distances equal to 2.44 and 2.41 Å, respectively).

The *in vacuo* Pd_7 cluster shows a large number of geometries, ranging from the pentagonal bipyramid to the face-capped octahedron.[26,28] The first, in the triplet spin state, was already presented in the literature as the most stable. However, as reported by Li *et al.*[25], distortions can occur due to the adsorption of small oxygenates, resulting in layered clusters similar to edge-capped octahedra. Indeed, upon the adsorption of the Pd_7 on the BNNT we found the same layered structure that, in the triplet state, resulted on the whole the most stable. This cluster is characterized by two layers (triangular and rhombic shaped) and, just for its peculiar symmetry, it was employed to demonstrate the interplay between the metal cluster and support surface geometry-matching with the metal

and support binding interaction ability. As a matter of fact, we found that the energy difference arising from adsorbing the rhombic or triangular face of the cluster on BNNT is only 5 kJ mol^{-1}, the more stable species (rhombic face interacting) showing an adsorption energy of 87.8 kJ mol^{-1}. Likely, the favorable energetic contribution due to the formation of four different Pd-N interactions, which is realized when the rhombic face is adsorbed (Figure 4a), is balanced by the higher complementarity between the B_3N_3 ring and the Pd_3 face, which occurs when the cluster adsorbs through the triangular face (Figure 4b). Eventually this leads to two nearly iso-energetic structures. The other two structures optimized in the singlet spin state are characterized by a distorted bipyramidal pentagonal geometry, that are *ca.* 80 kJ mol^{-1} less stable than the triplet state structures.

[Fig. 4 about here.]

To the best of our knowledge very few studies in the literature concern the complex Pd_8 cluster.[21] Among these, Zanti *et al.*[29] have studied its structure and interaction with CO, *in vacuo* at the B3LYP level. Thus, for the sake of comparison it is interesting to report the here optimized results at the CAM-B3LYP level. In agreement to previous studies, the Pd_8 species shows four different relevant geometries: the most stable has C_s symmetry and a quintet spin multiplicity. It is approximately isoenergetic to a C_2 structure, closely resembling a doubly capped octahedron. Furthermore, a D_{2d} and a C_s Pd_8 geometry can be also found approximately 30 and 50 kJ mol^{-1} higher in energy. Our calculations verify these geometries. However, one more C_{2v} geometry both with a triplet and quintet spin state was also found. This looks like a layered cluster with one five- and one three-atoms layer, having an arrangement closely resembling a fcc stacking plane disposition. The energetic differences specifying the most stable structures, which are always in the quintet spin state, are extremely small: the ground state shows the features of the C_s structure found by Zanti,[29] then the energy increases in the order D_{2d}, C_s and C_{2v}. These are almost isoenergetic, namely within 4 kJ mol^{-1}. The less stable structure is finally the C_2, which shows an energy 22 kJ mol^{-1} higher than that of the others. Reasonably, the found dissimilarities arise from the correction for the dispersion interactions provided by the CAM-B3LYP functional.

The optimization of the Pd_8/BNNT systems leads to the same C_s, C_{2v} and C_2 structures obtained *in vacuo*. Again the C_s structure (Figure 5a) is the most stable but an inversion of stability between the spin states occurs, with the triplet 21.5 kJ mol^{-1} more stable than the quintet. The adsorption energy between the Pd_8 cluster and the support is 72.6 kJ mol^{-1}. The same inversion was found for the C_{2v} structure of the supported species that actually is slightly more stable (12.5 kJ mol^{-1}) in the triplet than in the quintet spin state. This triplet state lies 28.6 kJ mol^{-1} higher than the C_s reference state. Due to its particular layered structure, the C_{2v} cluster might interact with BNNT through the three-atom layer (C_{2v}-up, Figure 5b) or the five-atom one (C_{2v}-bottom, Figure 5c). In the C_{2v}-up adsorption mode a distortion of the cluster from its original symmetry is evident, due to the interaction of the cluster with the nitrogen atoms of the BNNT support. Indeed, at least three Pd-N bindings can be evidenced, with a mean bond length of 2.4 Å, on the whole, contributing to an adsorption energy of 86.2 kJ mol^{-1}. Conversely, in the C_{2v}-bottom interaction mode, which shows an adsorption energy of 89.9 kJ mol^{-1}, the Pd atoms coordinate B-atop while the C_{2v} symmetry is preserved. Despite these differences, the two structures, in their most stable triplet state, are almost isoenergetic, differing by 4 kJ mol^{-1}.

It is worth to note that the energy differences calculated for the supported clusters are wider than for the unsupported ones. This is particularly evident if the supported C_2 Pd_8 structure is taken into account (Figure 5d): in the most stable quintet state, in fact, this structure is 44 kJ mol^{-1} less stable than the reference species, twice the difference found for the Pd_8 isolated structure. The reference state stabilization could be easily related to the fitting local connectivity occurring between the interacting face of the cluster and the BNNT surface atoms. In particular, three metallic atoms interact N-atop with one B_3N_3 ring while the fourth has an exocyclic bridge coordination, similar to that of the already described Pd_3 cluster. The Pd-N distances of 2.4 Å clearly witnesses strong Pd/BNNT interactions.

[Fig. 5 about here.]

3.1 Growth thermodynamics

The calculation of the cluster/support adsorption energy, although useful to investigate the desorption energetics, does not provide peculiar insights into the cluster growth process. The energetic analysis of the cluster growing is however a non trivial task that requires the definition of proper descriptors. With a simplified model, which can be exploited also to get information about the template effect of the BN nanotube, the growth of the Pd clusters onto the BNNT can be thought as a step-by-step process in which a metal atom (already adsorbed on BNNT) joins a preexisting BNNT supported cluster:

$$Pd_{n-1}/BNNT + Pd/BNNT \rightarrow Pd_n/BNNT$$

This model implies that the diffusion of a Pd atom moving on the BNNT surface should not be highly energy demanding. In order to support this hypothesis – and choosing among all the diffusion paths of one Pd atom on the hexagonal pattern of the BNNT surface – a hopping mechanism between adjacent N atop sites was studied. The process has actually

a negligible energy barrier (*ca.* 6 kJ mol^{-1}) associated with a transition state in which the metal atom is B-atop. Straightforwardly, this result validates the model proposed above, also suggesting that the growth process is only slightly affected by the initial distance between the preexisting Pd_{n-1} cluster and the incoming Pd atom on the support. Besides, if the palladium atom and cluster are far away from each other, the interaction energy, E^{int}, of the Pd atom with the BNNT is certainly not influenced by the presence of the Pd_{n-1} cluster on the same support, that is:

$$E^{int}(Pd|Pd_{n-1}/BNNT) \approx E^{int}(Pd/BNNT) \quad (2)$$

With this assumption we can calculate the energy associated with the nth growth step, ΔE_n^g, in terms of absolute energies, according to the equation:

$$\Delta E_n^g = E_{Pd_n/BNNT} - E_{Pd_{n-1}/BNNT} - E^{BSSE}_{Pd/BNNT} + E_{BNNT} \quad (3)$$

where $E_{Pd_n/BNNT}$ and $E_{Pd_{n-1}/BNNT}$ are the calculated absolute energies of the Pd_n/BNNT and Pd_{n-1}/BNNT systems and $E^{BSSE}_{Pd/BNNT}$ the energy of the Pd/BNNT system, containing the correction for the basis set superposition error. Of course, each contribution was referred to the BNNT supported system in its most stable spin state. Eq. 3 can be easily rearranged, obtaining:

$$\Delta E_n^g = \Delta E_n^{Ads} - \Delta E_{n-1}^{Ads} - \Delta E_{Pd}^{Ads} + \Delta E_v^g \quad (4)$$

where the ΔE_n^{Ads} terms are calculated using eq. (1) and ΔE_v^g, which corresponds to the expression $E_{Pd_n} - E_{Pd_{n-1}} - E_{Pd}$, is formed by terms referring only to the isolated metallic species. Finally, the constant term ΔE_{Pd}^{Ads} corresponds to the BSSE corrected adsorption energy of a Pd atom on the BNNT surface and is equal to -36.9 kJ mol^{-1}. From eq. (4), the energy of growth, ΔE_n^g, can be described as a sum of contributions, whose physical meaning has been already discussed earlier along the text. In particular, while the first three terms account for metal/support interactions, the last takes into account energetic contributions just related to Pd-Pd interactions, reflecting the energy released upon the addition *in vacuo* of a Pd atom to an isolated preexisting cluster. The calculated ΔE_n^g *vs.* n (being n the number of the Pd atoms in the cluster) are collected in Figure 6; other relevant quantities appearing in eq. (4) are reported as well. The trends of ΔE_n^g and ΔE_n^{Ads} show a quite good correlation. Both the curves, indeed, reach a minimum corresponding to Pd_4 and then slightly increase. This effect can be related to a substantial compensation of the terms ΔE_{n-1}^{Ads} and ΔE_v^g. Interestingly, except for the Pd_2 case, the energy released along the growth of a given sub-nanometric cluster is always greater than the energy released upon the adsorption of the same cluster.

[Fig. 6 about here.]

Analyzing the trend reported in Figure 6, it can be noticed that after Pd_5 the growth energy is within 100-130 kJ mol^{-1}. This would seem to suggest that a sort of plateau for ΔE_n^g is reached after the formation of a characteristic triangular metallic face on BNNT, as in the case of the Pd_6, Pd_7 and Pd_8 clusters. Noticeably, the structure of the adsorbed face of the Pd_n (n = 6, 7, 8) clusters does not evidence sensible distortions with respect to the corresponding face in the isolated clusters and, further, the Pd-Pd average bond lengths of these triangular faces (Pd_6, 2.74 Å, Pd_7 rhombic, 2.78 Å, Pd_7 triangular, 2.75 Å and Pd_8, 2.77 Å) are on the whole almost matching the value of the Pd-Pd distance (2.75 Å) found in the (111) surface, showed by appositely tailored Pd_{30} and Pd_{36} clusters, which were investigated at the B3LYP level in previous works.[30,31]

The curvature of the lattice might influence to a large extent surface phenomena as adsorption and growth processes. Analyzing the results reported in Figure 6, a turning point in the growth process seems to appear in-between the Pd_3 and Pd_4 clusters. In order to rationalize the possible influence of the curvature on the growth process, the geometric and energetic features of both Pd_3 and Pd_4 were evaluated when adsorbed on a (7,7) and on a (20,20) BNNT. Binding modes and preferred multiplicities resulted the same for both the clusters adsorbed on the differently curved BNNTs. Regarding the energetic of the growth process, it was found that in the (7,7) and (20,20) BNNTs the ΔE_n^g were -159.9 and -163.5 kJ mol^{-1}, respectively. These values are very close to that of the (12,12), that is -158.2 kJ mol^{-1}. Summarizing it seems that a very small contribution to the cluster growth process arises from the BN network curvature, as already found for other surface processes occurring on different nanotube systems.[32] Accordingly, it can be inferred that the palladium cluster growth on a zero curvature BN sheet could occur with the same features found for the BNNT used as model in the present work.

4 Conclusions

The interactions of sub-nanosized Pd clusters with a BNNT support were investigated, focusing both on the structural and energetic properties of the resulting systems. Different geometries and spin state multiplicities were taken into account. In some cases, namely Pd_2 and Pd_8, it was found that the interactions between the metal cluster and the BNNT support led to an inversion of the ground state multiplicity of the considered cluster. While in Pd_3/BNNT the triplet-singlet energy difference is reduced with respect to that calculated for the cluster *in vacuo*, in all other cases the whole Pd_n/BNNT system has the same multiplicity of the corresponding isolated Pd_n and shows large energy gaps with the other spin states. The growth of the Pd_n clusters would seem to be ruled by a templating effect of BNNT B_3N_3 rings. In fact, starting from the Pd_4 cluster,

the wide majority of the supported species showed triangular faces that effectively interact with the BNNT surface. For the same reason larger clusters showed stacked geometries with exposed (111)-like surfaces, thus suggesting the possibility to exploit BNNT supports as template scaffolds. As it is common for highly complex systems, each cluster has anyway its own peculiarity, arising from a delicate balance between Pd-Pd and Pd/BNNT interactions. However, since the average bond lengths in the supported and isolated clusters were pretty similar, it is possible to infer that establishing favorable Pd-N interactions is, on the whole, as important as retaining Pd-Pd interactions. This picture – reached through the calculation of the growth energy of the Pd clusters on the BNNT – also showed that the adsorption energy of the clusters is compatible with a strong physisorption process; anyway, the desorption of the formed cluster should not be highly energy demanding, opening interesting routes for novel synthesis of sub-nanometric metal particles with specific shapes.

References

1 M. H. Park, Y. Cho, K. Kim, J. Kim, M. Liu and J. Cho, *Angew. Chem. Int. Ed.*, 2011, **50**, 9647–9650.

2 B. Huang, H. X. Deng, H. Lee, M. Yoon, B. G. Sumpter, F. Liu, S. C. Smith and S. H. Wei, *Phys. Rev. X*, 2014, **4**, 021029.

3 C. Li, S. Yang, S.-S. Li, J.-B. Xia and J. Li, *J. Phys. Chem. C*, 2013, **117**, 483–488.

4 B. Bishnoi and B. Ghosh, *RSC Adv.*, 2013, **3**, 26153–26159.

5 M. Xu, T. Liang, M. Shi and H. Chen, *Chem. Rev.*, 2013, **113**, 3766–3798.

6 M. Terrones, J. M. Romo-Herrera, E. Cruz-Silva, F. López-Urías, E. Muñoz-Sandoval, J. J. Velázquez-Salazar, H. Terrones, Y. Bando and D. Golberg, *Mater. Today*, 2007, **10**, 30–38.

7 K. S. Kim, C. T. Kingston, A. Hrdina, M. B. Jakubinek, J. Guan, M. Plunkett and B. Simard, *ACS Nano*, 2014, **8**, 6211–6220.

8 M. Becton and X. Wang, *Phys. Chem. Chem. Phys.*, 2015, **17**, 21894–21901.

9 N. Gao and X. Fang, *Chem. Rev.*, 2015, **115**, 8294–8343.

10 G. Postole, A. Gervasini, C. Guimon, A. Auroux and B. Bonnetot, *J. Phys. Chem. B*, 2006, **110**, 12572–12580.

11 J. C. S. Wu and T. Y. Chang, *Catal. Today*, 1998, **44**, 111–118.

12 N. Meyer, D. Pirson, M. Devillers and S. Hermans, *Appl. Catal., A*, 2013, **467**, 463–473.

13 N. Meyer, M. Devillers and S. Hermans, *Catal. Today*, 2015, **241, Part B**, 200–207.

14 R. McCaffrey, H. Long, Y. Jin, A. Sanders, W. Park and W. Zhang, *J. Am. Chem. Soc.*, 2014, **136**, 1782–1785.

15 X. Wu and X. C. Zeng, *J. Chem. Phys.*, 2006, **125**, 044711.

16 M. J. Frisch, G. W. Trucks, H. B. Schlegel, G. E. Scuseria, M. A. Robb, J. R. Cheeseman, G. Scalmani, V. Barone, B. Mennucci, G. A. Petersson, H. Nakatsuji, M. Caricato, X. Li, H. P. Hratchian, A. F. Izmaylov, J. Bloino, G. Zheng, J. L. Sonnenberg, M. Hada, M. Ehara, K. Toyota, R. Fukuda, J. Hasegawa, M. Ishida, T. Nakajima, Y. Honda, O. Kitao, H. Nakai, T. Vreven, J. A. Montgomery, Jr., J. E. Peralta, F. Ogliaro, M. Bearpark, J. J. Heyd, E. Brothers, K. N. Kudin, V. N. Staroverov, R. Kobayashi, J. Normand, K. Raghavachari, A. Rendell, J. C. Burant, S. S. Iyengar, J. Tomasi, M. Cossi, N. Rega, J. M. Millam, M. Klene, J. E. Knox, J. B. Cross, V. Bakken, C. Adamo, J. Jaramillo, R. Gomperts, R. E. Stratmann, O. Yazyev, A. J. Austin, R. Cammi, C. Pomelli, J. W. Ochterski, R. L. Martin, K. Morokuma, V. G. Zakrzewski, G. A. Voth, P. Salvador, J. J. Dannenberg, S. Dapprich, A. D. Daniels, Ö. Farkas, J. B. Foresman, J. V. Ortiz, J. Cioslowski and D. J. Fox, *Gaussian 09 Revision D.01*, Gaussian Inc. Wallingford CT 2009.

17 S. Dapprich, I. Komáromi, K. S. Byun, K. Morokuma and M. J. Frisch, *J. Mol. Struct. THEOCHEM*, 1999, **461–462**, 1–21.

18 A. K. Rappe, C. J. Casewit, K. S. Colwell, W. A. Goddard and W. M. Skiff, *J. Am. Chem. Soc.*, 1992, **114**, 10024–10035.

19 S. Boys and F. Bernardi, *Mol. Phys.*, 1970, **19**, 553–566.

20 R. Koitz, J. K. Norskov and F. Studt, *Phys. Chem. Chem. Phys.*, 2015, **17**, 12722–12727.

21 A. Prestianni, F. Ferrante, E. M. Sulman and D. Duca, *J. Phys. Chem. C*, 2014, **118**, 21006–21013.

22 J. Zhang and A. N. Alexandrova, *J. Phys. Chem. Lett.*, 2012, **3**, 751–754.

23 G. Barone, D. Duca, F. Ferrante and G. La Manna, *Int. J. Quant. Chem.*, 2010, **110**, 558–562.

24 J. Moc, D. G. Musaev and K. Morokuma, *J. Phys. Chem. A*, 2003, **107**, 4929–4939.

25 S. J. Li, X. Zhou and W. Q. Tian, *J. Phys. Chem. A*, 2012, **116**, 11745–11752.

26 P. Liu, *J. Phys. Chem. C*, 2012, **116**, 25337–25343.

27 N. Meiyan and Z. Zhi, *J. Mol. Struct.: THEOCHEM*, 2009, **910**, 14–19.

28 M. Moseler, H. Häkkinen, R. N. Barnett and U. Landman, *Phys. Rev. Lett.*, 2001, **86**, 2545–2548.

29 G. Zanti and D. Peeters, *Eur. J. Inorg. Chem.*, 2009, **2009**, 3904–3911.

30 A. Prestianni, M. Crespo-Quesada, R. Cortese, F. Ferrante, L. Kiwi-Minsker and D. Duca, *J. Phys. Chem. C*, 2014, **118**, 3119–3128.

31 M. Crespo-Quesada, S. Yoon, M. Jin, A. Prestianni, R. Cortese, F. Cárdenas-Lizana, D. Duca, A. Weidenkaff and L. Kiwi-Minsker, *J. Phys. Chem. C*, 2015, **119**, 1101–1107.

32 R. Cortese, F. Ferrante, S. Roggan and D. Duca, *Chem. Eur. J.*, 2014, **21**, 3806–3814.

TOC entry

Boron Nitride Nanotubes as Template for Sub-Nanometric Palladium Clusters Growth

Roberto Schimmenti, Remedios Cortese, Francesco Ferrante, Antonio Prestianni, and Dario Duca

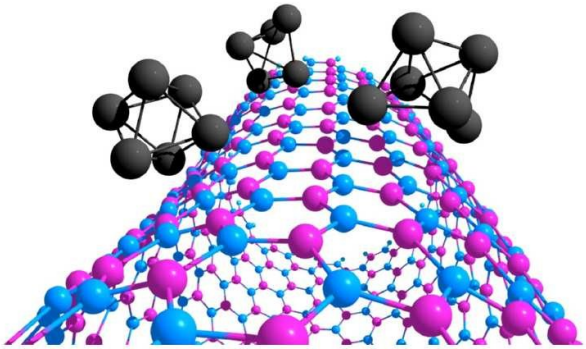

Keywords: Pd cluster growth, BNNT, DFT

Pd_2 bd / Å			Pd_3 bd / Å			Pd_4 bd / Å			
	M_s=0	M_s=1		M_s=0	M_s=1		N-atop	N-atop/BN-bridge	N-atop/N-atop
Pd1-Pd2	2.80	2.53	Pd1-Pd2	2.80	2.55	Pd1-Pd2	2.60	2.58	2.62
Pd1-N	2.30	2.54	Pd1-Pd3	2.82	2.65	Pd1-Pd3	2.69	2.74	2.76
Pd2-N	2.43	2.54	Pd2-Pd3	2.90	2.66	Pd1-Pd4	2.71	2.73	2.59
Pd2-B	2.30	—	Pd1-N	2.39	2.38	Pd2-Pd3	2.57	2.56	2.54
			Pd1-B	2.43	—	Pd2-Pd4	2.57	2.60	2.63
			Pd2-N	2.38	2.38	Pd3-Pd4	2.70	2.71	2.77
			Pd2-B	2.39	—	Pd1-N	2.38	2.58	2.46
			Pd3-N	2.48	—	Pd4-B	—	2.57	2.89
			Pd3-B	2.32	—	Pd4-N	—	—	2.46

Table 1 Bond distance (bd) values, characterizing the adsorbed cluster geometries in the Pd_2/BNNT (singlet and triplet states), Pd_3/BNNT (singlet and triplet states) and Pd_4/BNNT (triplet state, in different configurations) systems

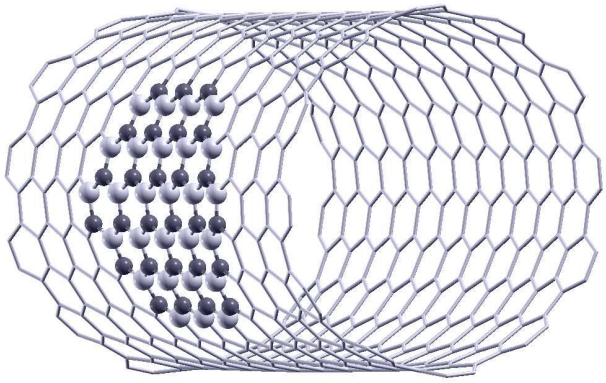

Fig. 1 Optimized (12,12) single walled armchair BNNT geometry: the model system used in the QM/MM ONIOM approach is highlighted by balls and sticks.

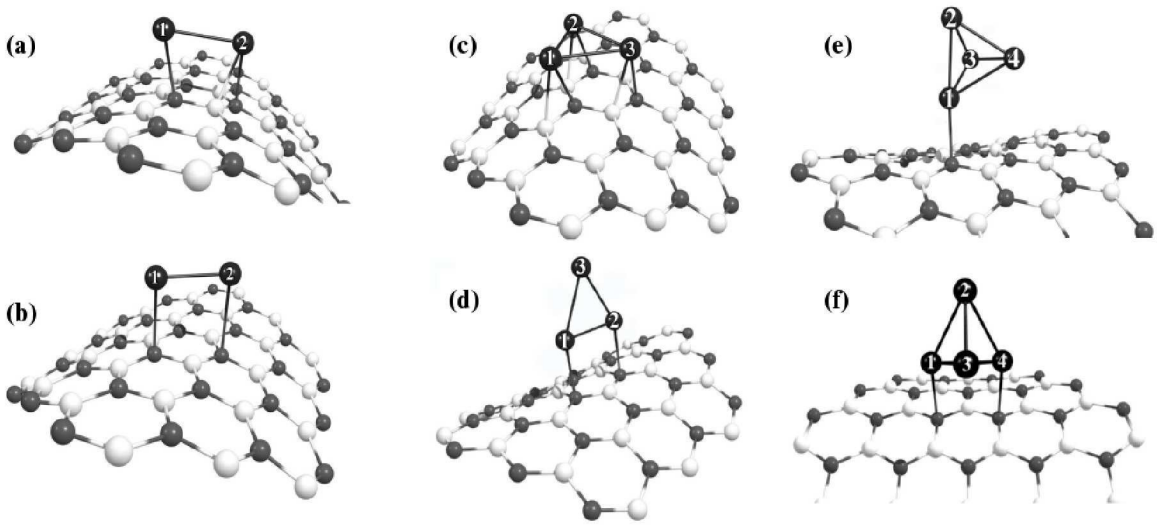

Fig. 2 Optimized structures of BNNT supported palladium clusters: Pd_2/BNNT in the (a) singlet and (b) triplet spin state, Pd_3/BNNT in the (c) singlet and (d) triplet spin state and Pd_4/BNNT with (e) N-atop and (f) N-atop/N-atop coordination.

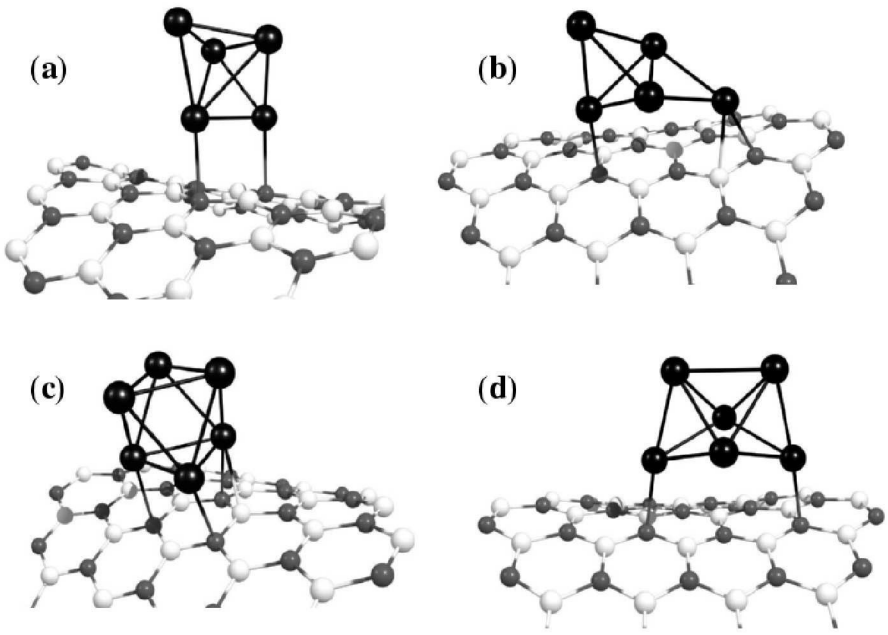

Fig. 3 Optimized structures of the BNNT supported Pd_5 and Pd_6 clusters: Pd_5/BNNT (a) trigonal bipyramidal and (b) edge-capped tetrahedral geometries, Pd_6/BNNT (c) octahedral and (d) C_{2v} distorted octahedral geometries.

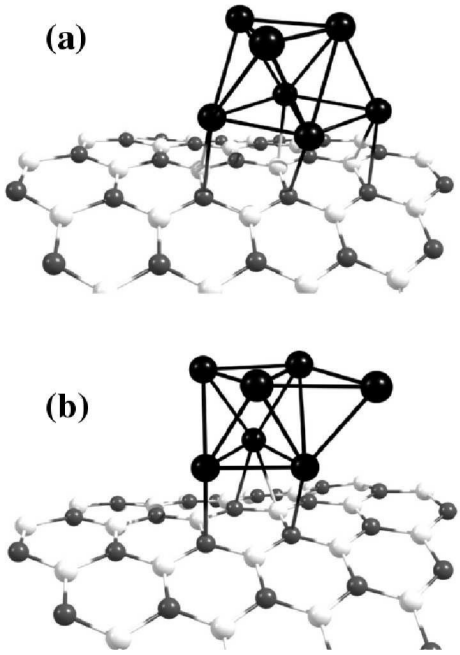

Fig. 4 Optimized structures of the BNNT supported Pd_7 layered cluster, adsorbed through (a) the rhombic and (b) the triangular face.

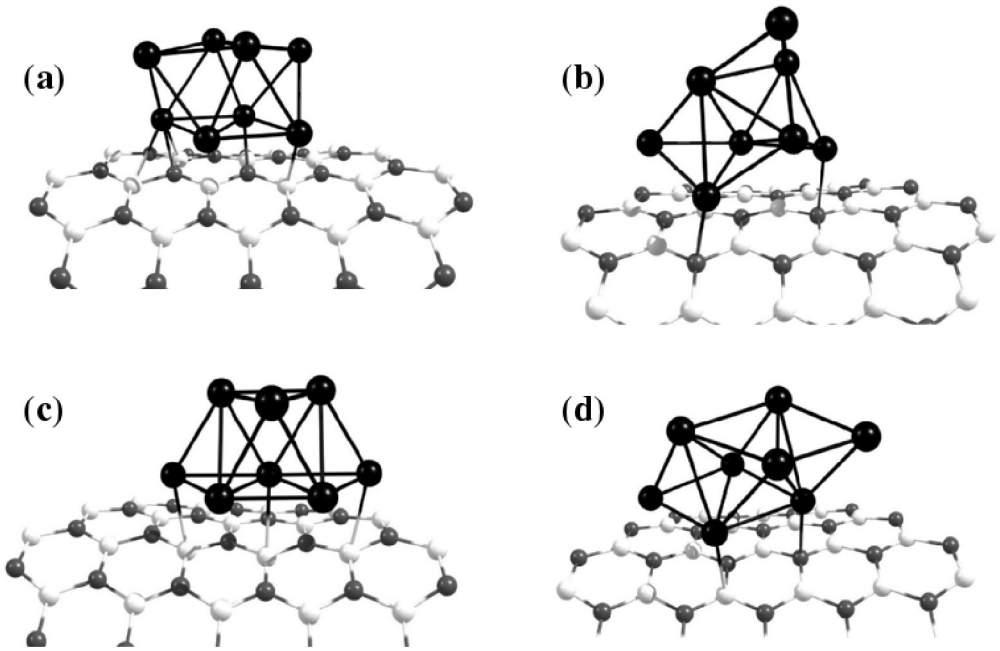

Fig. 5 Optimized structures of the supported Pd_8/BNNT cluster: (a) the most stable C_s structure, (b) and (c) C_{2v}-up and C_{2v}-bottom mode of adsorption, (d) quintet multiplicity C_2 structure.

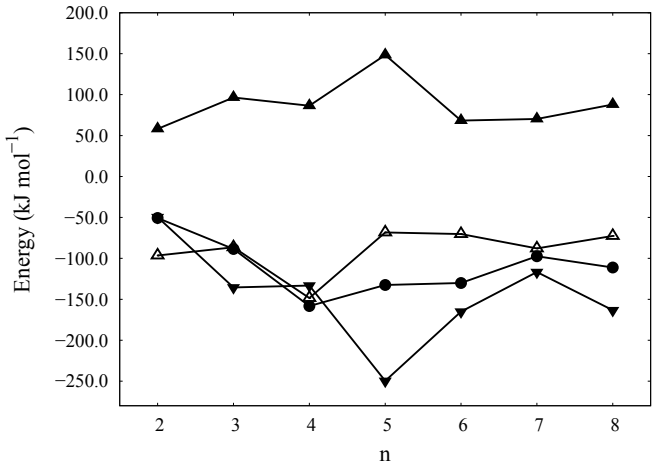

Fig. 6 Energy of growth and related energetic contributions characterizing the Pd_n/BNNT systems for different n: filled circles, ●, represent the ΔE_n^g values obtained by eq. (4); empty, △, filled up, ▲, and down, ▼, triangles illustrate various contributions (ΔE_n^{Ads}, $-\Delta E_{n-1}^{Ads}$ and ΔE_v^g, respectively) to the ΔE_n^g terms. The other two terms in eq. (4), ΔE_1^{Ads} and ΔE_{Pd}^{Ads}, are -58.6 and -36.9 kJ mol^{-1}, respectively.